Rare Metal Materials and Engineering
Volume 52, Issue 8, August 2023
Available online at www.rmme.ac.cn

Science Press

Cite this article as: Tong Wenhui, Huang Bonan, Sun Bowei, et al. Effect of Er-Ba Composite Modification on Microstructure and Mechanical Properties of Mg-2.5Si-4Zn Cast Alloy[J]. Rare Metal Materials and Engineering, 2023, 52(08): 2683-2692.

ARTICLE

Effect of Er-Ba Composite Modification on Microstructure and Mechanical Properties of Mg-2.5Si-4Zn Cast Alloy

Tong Wenhui, Huang Bonan, Sun Bowei, Wang Jie, Bai Yufei

School of Materials Science and Engineering, Shenyang Aerospace University, Shenyang 110136, China

Abstract: The enhanced phase Mg_2Si in the magnesium alloy can significantly improve the hardness, wear resistance, especially high temperature creep resistance. But the Mg_2Si phase of the as-cast hyper-eutectic Mg-Si alloy will seriously cut the alloy matrix because of the coarse angular shape of the primary Mg_2Si and complex Chinese script morphology of the eutectic Mg_2Si. In order to improve the properties of Mg-2.5Si-4Zn alloy, the modification experiments of adding Er/Er-Ba were performed and the effects on the alloy microstructure and Mg_2Si phase were investigated by the optical microscopy (OM), scanning electron microscopy (SEM), energy dispersive spectrometry (EDS) and X-ray diffractometer (XRD). The mechanical properties were measured and analyzed by the computer-aided electric-loaded tensile tester. The results show that with the addition of 0.6wt% Er to the Mg-2.5Si-4Zn alloy, the primary Mg_2Si in the microstructure transforms from a coarse dendritic shape into a regular tetragonal block shape, while the eutectic Mg_2Si transforms from a coarse Chinese script type to a more complex short rod shape. When adding 0.8wt% Ba subsequently, the primary Mg_2Si further transforms from a regular tetragonal bulk shape to an irregular fine bulk shape with grooves and holes, and the eutectic Mg_2Si has an obvious refining effect and is diffusely distributed with the dot/short-line shape in the alloy matrix. The best metamorphic effect is obtained by adding 0.6wt% Er and 0.8wt% Ba. The mechanical properties of the Mg-2.5Si-4Zn alloy modified by Er-Ba composite modifier are significantly improved, with the tensile strength σ_b and elongation δ increasing to 168 MPa and 5.04%, respectively.

Key words: Mg-Si-Zn alloy; Mg_2Si; microstructure; composite modification; mechanical properties

Magnesium alloy has a broad development prospect in the fields of automobile production and aerospace because of its low density, high specific strength and good vibration dissipation, etc. However, the wide application of magnesium alloy has been limited due to the lack of alloy strength and thermal stability at high temperature and poor corrosion resistance [1–3].

In the study of Mg alloying, it is found that the enhanced phase Mg_2Si formed by element Si and Mg has high hardness, high melting point and high elastic modulus, which can significantly improve the hardness, wear resistance and high temperature creep resistance of magnesium alloy and refine the alloy matrix to a certain extent, showing better research and application prospects[4–6].

In spite that the Mg-Al-Si alloy shows better creep resistance than the Mg-Al alloy without Si, its application is limited because the intermetallic $Mg_{17}Al_{12}$ phase in the alloy's microstructure has poor high-temperature stability[7]. The Mg-Si-Zn alloy, completely free of Al, can not only avoid the generation of $Mg_{17}Al_{12}$ phase, but also further reduce the cost[8–9]. But the matrix of the as-cast Mg-Si alloy is cut by the primary and eutectic Mg_2Si in the solidified microstructure because of their coarse and complex morphology, which seriously deteriorates the mechanical properties of the magnesium alloy [10]. Therefore, controlling the size and improving morphology of Mg_2Si, which can significantly improve the mechanical properties of magnesium alloys, has become one of the hot topics in the research on magnesium alloys containing Si [11].

At present, researchers usually use hot extrusion, rapid solidification, and modification treatment[12–16] to improve the microstructure of Si-containing Mg alloys, among which the addition of various trace elements (such as Sr[17], Sb[18–19], Ca[20], Er[21], Y[21–22]) to modify Mg_2Si has been studied more

Received date: February 27, 2023
Foundation item: Scientific Research Fund of Liaoning Provincial Education Department (CN) (JYT2020079)
Corresponding author: Tong Wenhui, Ph. D., Associate Professor, School of Materials Science and Engineering, Shenyang Aerospace University, Shenyang 110136, P. R. China, Tel: 0086-24-89728968, E-mail: 20140013@sau.edu.cn

and more. Srinivasan[18] and Yang[19] et al reported that Sb can transform Mg_2Si from Chinese character shapes to fine polygonal shapes and the comprehensive mechanical properties of magnesium alloys are significantly improved. Song[20] et al found that Ca has good modification effect on eutectic Mg_2Si in Mg-Si-Zn alloy, and makes eutectic Mg_2Si diffuse and fine. Jiang[22] et al studied the modification effect of Y in Mg-5Si alloy and found that Y has good modification effect on both primary and eutectic Mg_2Si.

Ba also has a good modified effect on Mg_2Si[23–24]. Chen[25] et al investigated the effect of Ba-Sb composite modification on Mg-5Si alloy, and the results showed that with the simultaneous addition of Ba and Sb modifying agents, the refinement of primary Mg_2Si is significant and the morphology changes from coarse dendrites to fine polygons, and the Ba_2Sb compound is thought to be the heterogeneous nucleation core of primary Mg_2Si.

For the Si-containing magnesium alloy, the addition of Er or Ba presents a good modification effect, but the study of Er and Ba composite modification in the hyper-eutectic Mg-Si alloy has been scarcely found to be carried out. In this study, for the Mg-2.5Si-4Zn alloy, the effects of Er-Ba composite modification on the microstructure and mechanical properties were investigated and the modification mechanism of two modifiers and their interaction were also revealed. The content of modifiers was optimized to improve the morphology and to refine the size of the primary phase and eutectic Mg_2Si microstructure.

1 Experiment

1.1 Alloy composition design and alloy melting

In order to investigate the effect of Er and Ba elements on the microstructure and mechanical properties, in the experiment, the alloy composition was designed by the addition of different content of Er or Ba, based on the Mg-2.5Si-4Zn alloy, as shown in Table 1.

The alloy specimens were prepared by melting and casting according to the alloy composition ratios shown in Table 1, using industrial pure magnesium (99.9wt%), pure zinc (99.9wt%), Mg-10Si master alloy, Mg-20Er master alloy and Mg-10Ba master alloy as raw materials. The melting and casting experiments were performed using the SG-7.5-12 atmospheric-well type resistance furnace equipped with a homemade device mixing shielding gas as follows.

1) When the resistance furnace was heated up to 500 °C and held, pure magnesium was added to the crucible in the furnace. At the same time, the mixture of CO_2 and SF_6 gas, with a volume ratio of 100∶1, from a homemade gas mixing device, was passed into the crucible for protecting magnesium alloy at high temperatures. And then the resistance furnace was continuously heated.

2) When the furnace temperature was rasied to 750 °C for holding, the pure magnesium in the crucible was gradually melt. After the pure magnesium was completely melted for about 30 min, the weighed Mg-10Si alloy was added to the magnesium liquid in batches and stirring was carried out every 30 min until the Mg-10Si alloy was thoroughly melted to ensure the uniform composition of alloy melt.

3) After above, Zn and the modifiers of Er or Ba were added to the magnesium alloy melt; then the melt was stirred and held for 5–10 min.

4) Finally, the slag on the surface of the melt was removed and the melt was refined using RJ-5 type refining agent. After 5 min, the melt was poured into a cylindrical graphite casting mold at 150 °C to obtain alloy specimens with dimensions of Φ50 mm×100 mm.

Table 1 Chemical composition of Mg-2.5Si-4Zn-*x*Er-*y*Ba alloys (wt%)

Alloy No.	Si	Zn	Er	Ba	Mg
1	2.5	4	0	0	Bal.
2	2.5	4	0.4	0	Bal.
3	2.5	4	0.6	0	Bal.
4	2.5	4	0.8	0	Bal.
5	2.5	4	1.0	0	Bal.
6	2.5	4	1.2	0	Bal.
7	2.5	4	0.6	0.5	Bal.
8	2.5	4	0.6	0.8	Bal.
9	2.5	4	0.6	1.0	Bal.
10	2.5	4	0.6	1.2	Bal.
11	2.5	4	0.6	1.5	Bal.
12	2.5	4	0.6	2.0	Bal.

1.2 Analysis and test methods

Metallographic specimens were cut from the middle of the alloy ingot perpendicular to its axis direction, then ground and polished, and etched with 0.4vol% HNO_3 alcohol solution, after which the specimen surface was cleaned with anhydrous ethanol.

The microstructure of alloy specimens was observed by metallographic microscopy (Olympus OM) and scanning electron microscopy (SEM), the micro-zone composition was measured and analyzed by energy dispersive spectroscopy (SEM-EDS) and phase discrimination and identification were conducted by X-ray diffractometer (XRD). The room-temperature properties were measured by RG3050 computer-aided electric-loaded tensile tester. The effect of Er, Ba on the modification mechanism of the primary Mg_2Si and the eutectic Mg_2Si in the Mg-2.5Si-4Zn alloy and the interaction of the compound modification were analyzed and revealed, and the addition of Er and Ba elements in the alloy was optimized according to the obtained results.

2 Results and Discussion

2.1 Effect of Er on solidification structure of Mg-2.5Si-4Zn alloy

Different amounts of Er were added into the Mg-2.5Si-4Zn magnesium alloy melt (0wt% , 0.4wt% , 0.6wt% , 0.8wt% , 1.0wt% , and 1.2wt%), and the obtained microstructure is

shown in Fig.1. The average area of primary Mg_2Si grains and eutectic Mg_2Si with different Er contents is shown in Fig.2. It can be seen from Fig.1 that the metallographic microstructure of the Mg-2.5Si-4Zn alloy specimen is mainly composed of α-Mg, primary Mg_2Si, eutectic Mg_2Si and eutectic MgZn.

As shown in Fig.1a–1c and Fig.2, the size of the primary and eutectic Mg_2Si gradually decreases and the morphology is improved with increasing the content of Er from 0wt% to 0.6wt%. The primary Mg_2Si changes from dendrites with 30–40 μm in length, 10–20 μm in width and 420 μm^2 in the average area to fine quadrilateral blocks with the diagonal length of 10–30 μm and the average area of about 181 μm^2, and the eutectic Mg_2Si breaks down from a complex Chinese script shape with the average area of about 390 μm^2 into a more complex short-rod shape with the average area of about 157 μm^2.

When the addition of Er exceeds 0.6wt% at less than 1.2wt%, the size of primary and eutectic Mg_2Si starts to increase, while the primary Mg_2Si changes from a regular flat rectangular block to the irregular polygon shape with pores, and the eutectic Mg_2Si regrows from the short rod-like microstructure to the more complex Chinese script shape. Therefore, addition of 0.6wt% Er element into the magnesium alloy has the best modification effect on the primary and eutectic Mg_2Si.

Further, Fig.3 shows the statistical size distribution of the primary Mg_2Si of the magnesium alloy added with 0.6wt% of the Er element, where the histogram shows the frequency of primary Mg_2Si grain in each size interval, the red shows the fitted curve, and the blue is the cumulative frequency curve. As shown in Fig.3, the primary Mg_2Si grain size is 11.93 μm, with an arithmetic mean of 12.61 μm.

The modification mechanism of Er element in Mg-2.5Si-4Zn alloy was analyzed by the SEM results (Fig.4) and XRD (Fig.5). Combining the EDS result with XRD patterns, it can be identified that the Mg_2Si and MgZn in the alloy appear.

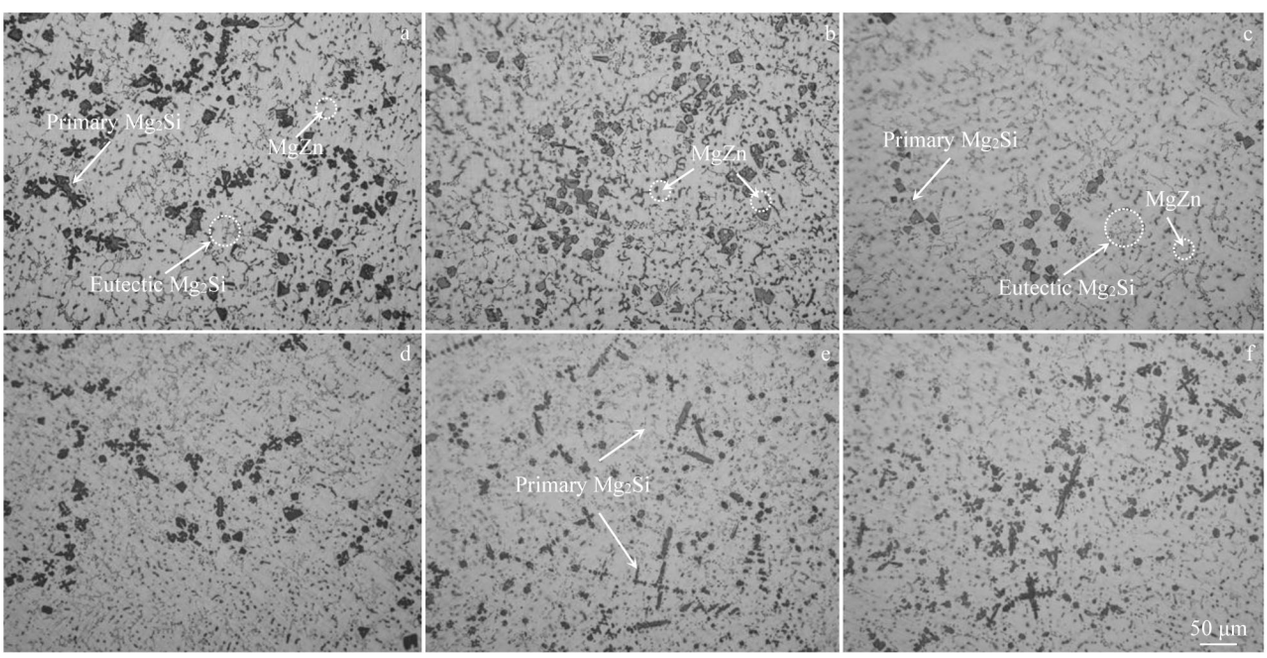

Fig.1 Effect of Er content on solidification microstructure of Mg-2.5Si-4Zn alloy: (a) 0wt%, (b) 0.4wt%, (c) 0.6wt%, (d) 0.8wt%, (e) 1.0wt%, and (f) 1.2wt%

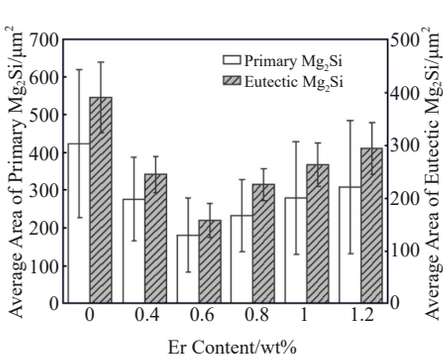

Fig.2 Average area of primary Mg_2Si grains and eutectic Mg_2Si with different Er contents

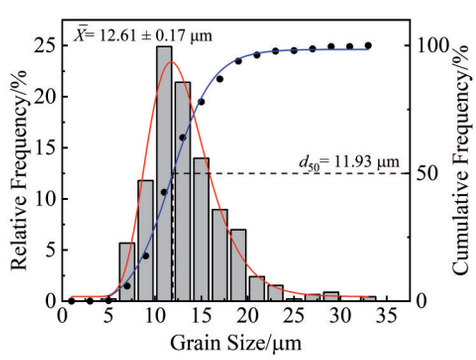

Fig. 3 Primary Mg_2Si grain size statistics of Mg-2.5Si-4Zn-0.6Er alloy

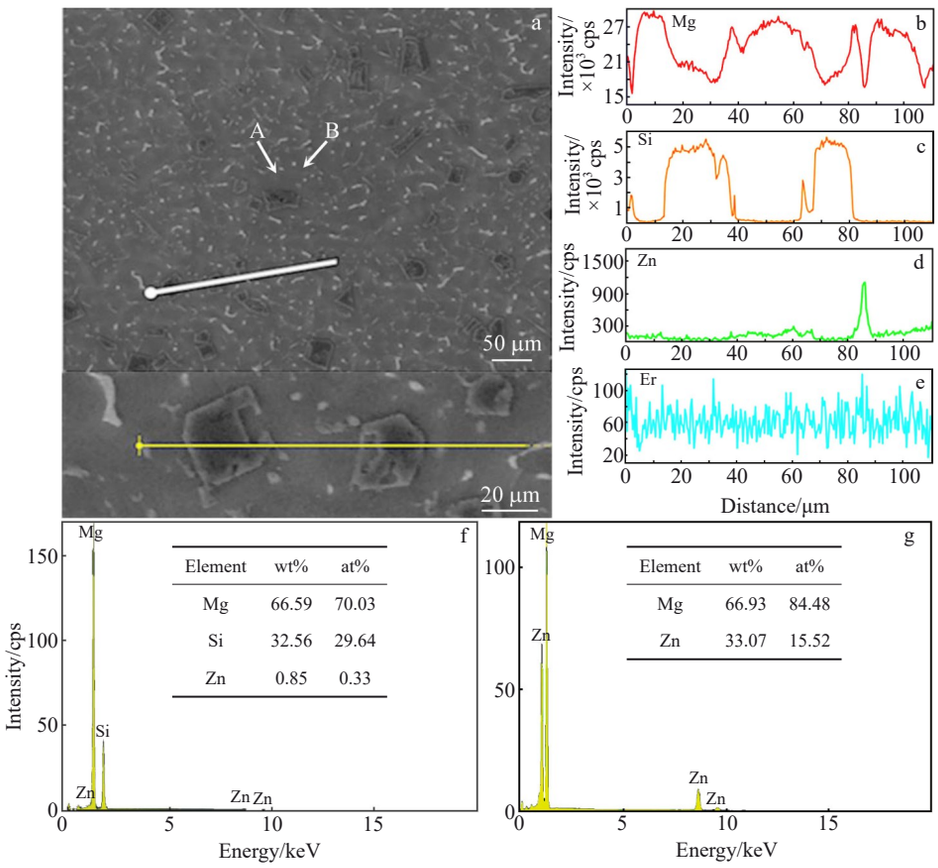

Fig.4 Analysis of modification mechanism of Er element in Mg-2.5Si-4Zn-0.6Er alloy: (a) SEM image; (b–e) element distributions of Mg, Si, Zn and Er along the line marked in Fig.4a; (f) EDS result of point A; (g) EDS result of point B

From Fig. 4, it can be seen that the Er content is higher near the primary and eutectic Mg_2Si. It can be deduced that during the solidification of the alloy melt, Er elements enrich on the surface of the primary Mg_2Si and "occupy" the non-close-packed growth interface[26], which makes the growing atoms of Mg_2Si cannot effectively adhere to the atom position of the crystal surface, slowing down the rapid growth of the primary Mg_2Si in the preferred growth direction, and turning the dendritic primary Mg_2Si into small rectangular lumps.

Similarly, the element of Er can also accumulate at the growth front of eutectic Mg_2Si when it grows and inhibits the anisotropic growth of eutectic Mg_2Si. So, the eutectic Mg_2Si with the complex multi-stroke Chinese script shape is transformed into the more complex short rod-like one.

But Er in the Mg-2.5Si-4Zn alloy melt may react with Mg or Si to form Mg-Er or Er-Si compounds when the adding amount of Er is higher than 0.6wt% due to the high chemical activity of the rare earth element Er and its low solid solubility in magnesium alloys. It is well-known that the smaller the electronegativity difference between the two elements, the easier to form a solid solution or a compound[27]. The electronegativities of Mg, Si and Er are 1.31, 1.8 and 1.22, respectively. So, Er prefers to react with Si to form Er_xSi_y compounds[28] because the electronegativity difference between Er and Si (0.58) is much larger than that between Er and Mg (0.09). Combined with Fig. 5, it can be identified that

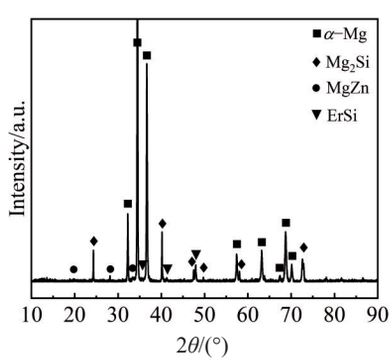

Fig.5 XRD pattern of Mg-2.5Si-4Zn-1.2Er alloy

the compound between Er and Si is ErSi.

According to the classical theory of nucleation, increasing the concentration of Er in the alloy melt can induce enough constituent fluctuations to generate ErSi nuclei. Once the crystal nuclei appear in the melt, their rapid growth will consume a large number of Er and Si atoms, making the Er modification effect weakened. Therefore, when the addition of Er in the alloy melt exceeds the optimum content of 0.6wt%, an over-modified effect occurs as the Er content continues to increase, i.e. the size of primary Mg_2Si phase increases and its morphology turns back to coarse dendrites, while the morphology of the eutectic Mg_2Si tends back to complex Chinese script shape.

2.2 Effect of Ba addition on solidified microstructure of Mg-2.5Si-4Zn-0.6Er alloy

2.2.1 Solidified microstructure

On the basis of the optimal result from the previous experiments, the Er-Ba composite modification was performed with different addition amounts of Ba. Fig.6 shows the solidified microstructure of the Mg-2.5Si-4Zn-0.6Er alloy with different addition amounts of Ba. The eutectic Mg_2Si in the microstructures of Mg-2.5Si-4Zn-0.6Er alloy is magnified, as shown in Fig. 7. Fig. 7a presents the details of eutectic Mg_2Si at different magnifications in the microstructure of Mg-2.5Si-4Zn-0.6Er alloy and Fig. 7b presents the details of eutectic Mg_2Si after adding the element Ba to Mg-2.5Si-4Zn-0.6Er alloy. Fig. 8 shows the average area of primary Mg_2Si grains and eutectic Mg_2Si with different Ba contents.

Combining Fig. 6, Fig. 1c and Fig. 8, it can be seen that the primary Mg_2Si is changed from a regular tetragonal block to an irregular polygonal block with holes and grooves and its size decreases a little with the increase in addition amount of Ba within 0.8wt%, and it gradually changes back to a coarse irregular dendritic shape and increases obviously in size when the Ba addition increases from 0.8wt%.

In addition, from Fig. 6, the eutectic Mg_2Si is changed from a more complex short rod shape to a fine dot-rod shape with the increase in Ba addition content, which can be seen more clearly from Fig. 7, and the grain size gradually decreases, but not obviously.

Thus, when 0.6wt% of Er and 0.8wt% of Ba are added to the Mg-2.5Si-4Zn alloy, the modification effect of primary and eutectic Mg_2Si is the best, as seen from Fig.6 and Fig.8, in which the primary Mg_2Si becomes an irregular polygonal block shape with an average area of about 124 μm^2 and the eutectic Mg_2Si has a simple dot-rod shape with an average area of about 69 μm^2.

Fig. 9 shows the statistical frequency distribution of the primary Mg_2Si grain size of the magnesium alloy, in which 0.6wt% of Er element and 0.8wt% of Ba element are added.

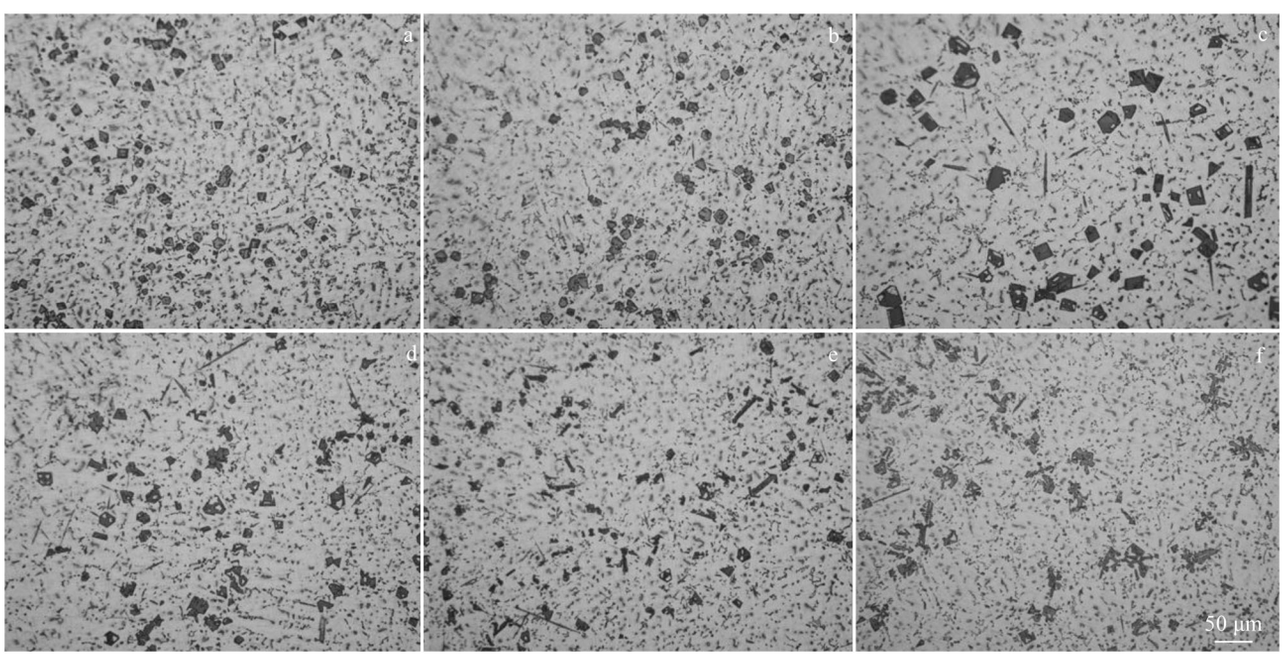

Fig.6 Microstructures of solidified Mg-2.5Si-4Zn-0.6Er alloy with different Ba contents: (a) 0.5wt%, (b) 0.8wt%, (c) 1.0wt%, (d) 1.2wt%, (e) 1.5wt%, and (f) 2.0wt%

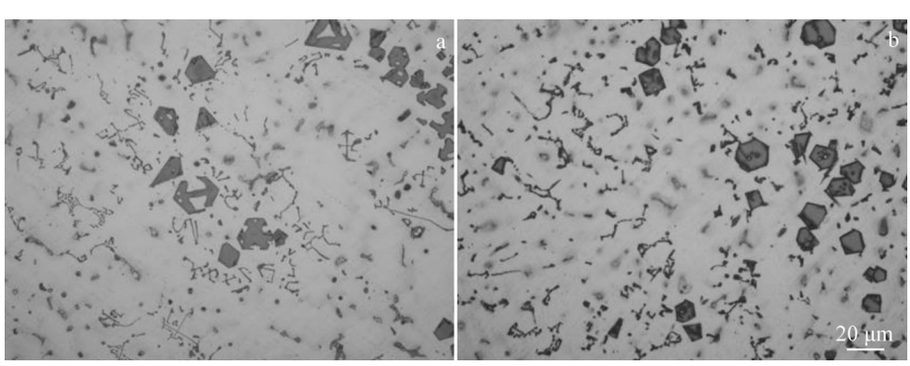

Fig.7 Eutectic Mg_2Si in the as-cast Mg-2.5Si-4Zn-0.6Er alloy without Ba addition (a) and after Ba addition (b)

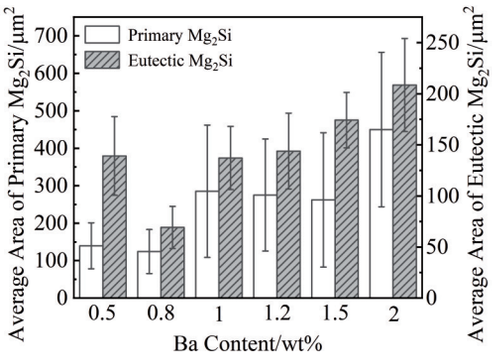

Fig.8 Average area of primary Mg_2Si grains and eutectic Mg_2Si with different Ba contents

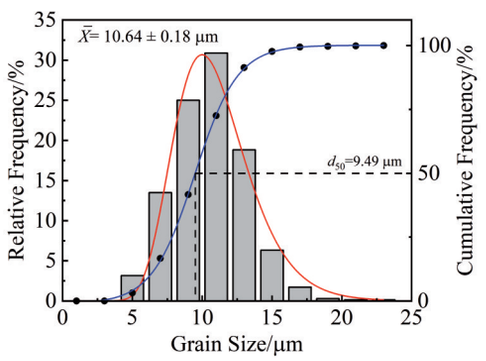

Fig.9 Primary Mg_2Si grain size statistics of Mg-2.5Si-4Zn-0.6Er-0.8Ba alloy

The histogram shows the frequency of primary Mg_2Si grain in each size interval, the red curve is fitted data, and the blue one is the cumulative frequency. The primary Mg_2Si grain size is 9.49 μm, with an arithmetic mean of 10.64 μm.

2.2.2 Er-Ba composite modification

In order to investigate the mechanism of composite modification of adding Er-Ba to the magnesium alloy, the SEM observation and XRD analysis of Mg-2.5Si-4Zn-0.6Er-1.2Ba alloy were carried out, as shown in Fig. 10 and Fig. 11. The EDS results of Fig. 10b shows that the acicular phase marked in Fig. 10a contain different contents of Ba, Mg and Si, indicating that the phase is Ba-Mg-Si compound. Further, the $BaMg_2Si_2$ phase is detected in the XRD pattern as shown in Fig. 11. Combining the EDS detection result with XRD pattern, it can be inferred that the acicular compound is $BaMg_2Si_2$ in the alloy.

The modification effect intensifies with the addition of the Ba modifier to the Mg-2.5Si-4Zn-0.6Er alloy, presumably because the generated $BaMg_2Si_2$ acts as a heterogeneous nucleation core for the primary Mg_2Si, which increases the nucleation rate of the primary Mg_2Si and suppresses the growth.

In order to confirm this conjecture, i. e. the $BaMg_2Si_2$ compounds becomes the cores for Mg_2Si nucleation, the low-index plane matching the compounds with Mg_2Si can be calculated according to the following Bramfitt ' s lattice

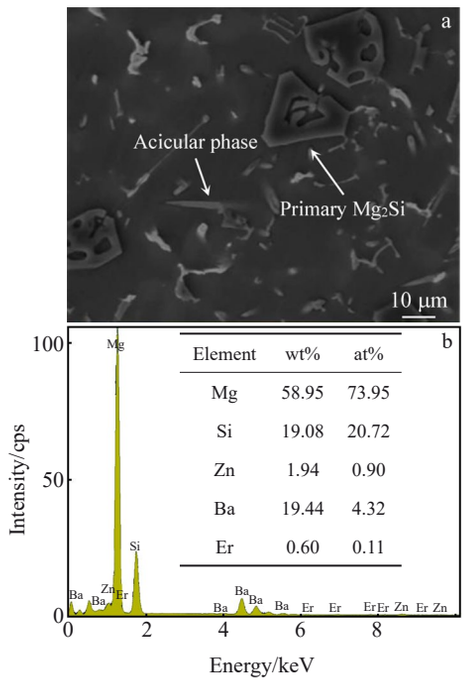

Fig.10 SEM image of Mg-2.5Si-4Zn-0.6Er-1.2Ba alloy (a) and EDS result of acicular phase (b)

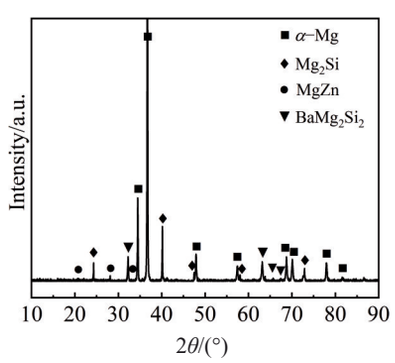

Fig.11 XRD pattern of Mg-2.5Si-4Zn-0.6Er-1.2Ba alloy

mismatch equation[29]:

$$\delta_{\frac{(hkl)_s}{(hkl)_n}} = \frac{1}{3}\sum_{i=1}^{3}\frac{\left|d[uvw]_s^i\cos\theta - d[uvw]_n^i\right|}{d[uvw]_n^i} \times 100\% \quad (1)$$

where $(hkl)_s$ is a low-index plane of the substrate, $[uvw]_s$ is a low-index direction in $(hkl)_s$, $d[uvw]_s$ is the interatomic spacing along $[uvw]_s$; $(hkl)_n$ is a low-index plane of the nucleated crystal, $[uvw]_n$ is a low-index direction in $(hkl)_n$, $d[uvw]_n$ is the interatomic spacing along $[uvw]_n$; θ is the angle between $[uvw]_s$ and $[uvw]_n$ ($\theta<90°$)[30].

According to the Bramfitt's lattice mismatch equation [29], only when the mismatch between the substrate and the crystalline phase is $\delta < 15\%$, it is possible to become a heterogeneous nucleation core of the crystalline phase. If the mismatch is $\delta< 6\%$, it can be a more effective heterogeneous nucleation core. The spatial lattice structure of Mg_2Si and $BaMg_2Si_2$ are face-centered cubic and simple tetragonal, respectively. There are the same atomic arrangement and close

atomic spacing between the low-index plane (001) of Mg_2Si and the low-index plane (001) of $BaMg_2Si_2$, as shown in Fig. 12. It is calculated out from the data in Fig. 12 according the Bramfitt's lattice mismatch equation that the lattice mismatch of the two is 3.01%[31]. Therefore, the $BaMg_2Si_2$ compound can become a heterogeneous nucleation core of Mg_2Si.

Further, in the experiment, from the line scanning results (Fig. 13), it can be found that not only the elements of Mg and Si but also Ba appear near the centers of three crystal blocks of A, B and C (marked in Fig. 13a) of Mg_2Si (the specific positions pointed by the blue arrows in Fig. 13b – 13f), by which it can be proved that $BaMg_2Si_2$ compound is positioned at the core of Mg_2Si crystal.

Therefore, as shown in Fig. 13, it is inferred from the EDS line scan results and the Er-Ba phase diagram that no

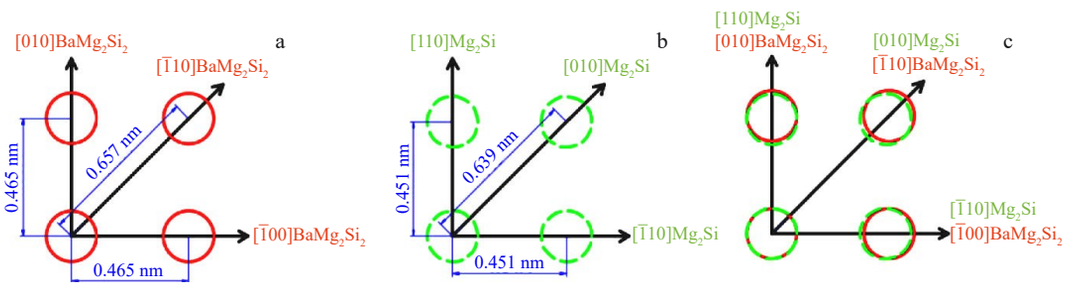

Fig.12 Schematic diagrams of lattice mismatch between $BaMg_2Si_2$ and Mg_2Si: (a) atomic arrangement of $BaMg_2Si_2$ on (001) lattice plane, (b) atomic arrangement of Mg_2Si on (001) lattice plane, and (c) matching relationship between atoms of $BaMg_2Si_2$ on (001) lattice plane and Mg_2Si on (001) lattice plane

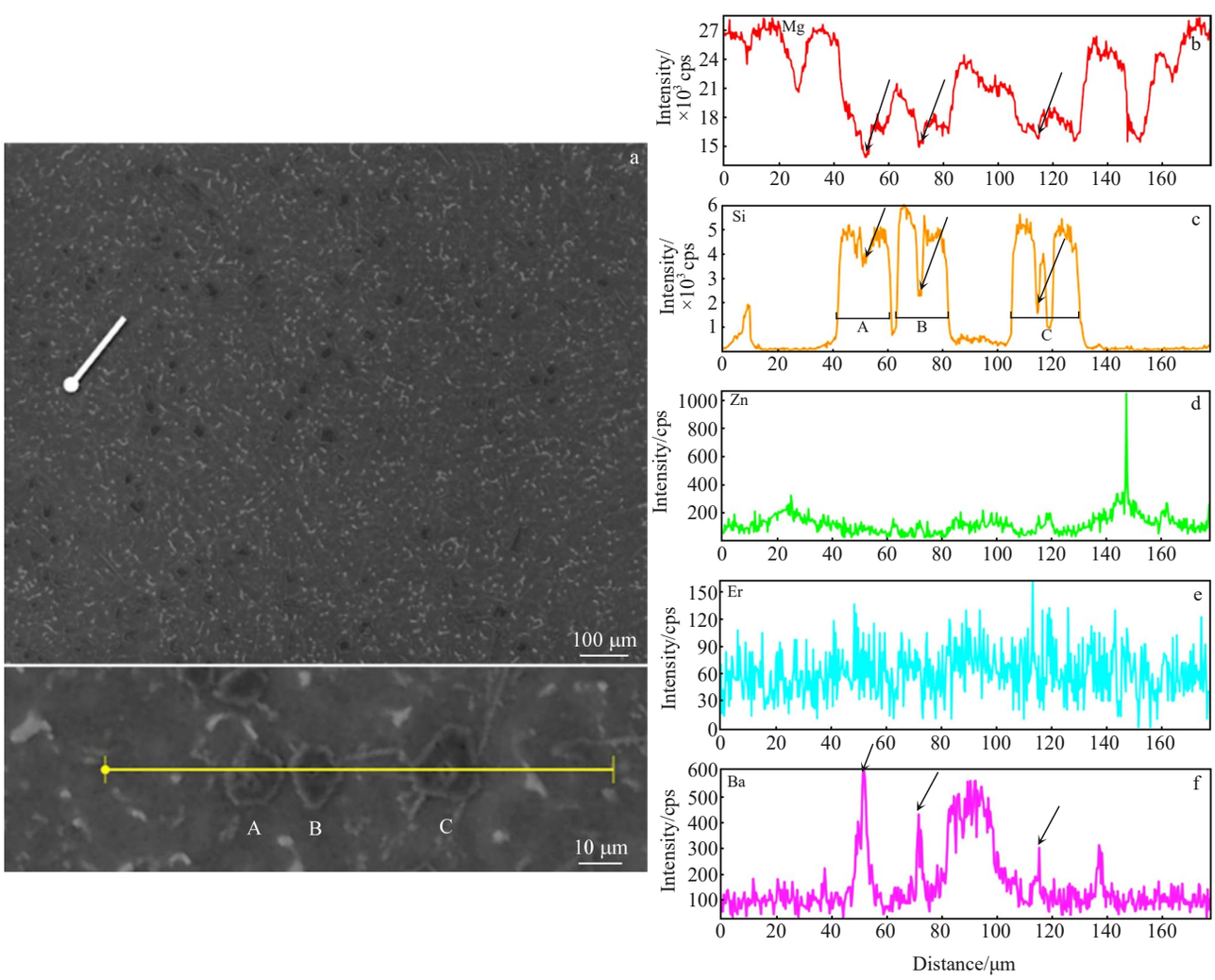

Fig.13 SEM images (a) and EDS line scanning results of element Mg (b), Si (c), Zn (d), Er (e) and Ba (f) along marked line in Fig. 13a for Mg-2.5Si-4Zn-0.6Er-1.2Ba alloy

compounds are generated between Er and Ba, and the composite modification mechanism of Er-Ba is as follows.

At the stage of initiating the solidification of the alloy melt after adding Er-Ba modifier, the $BaMg_2Si_2$ compound first formed in the melt acts as a nucleation substrate for the primary Mg_2Si to promote the heterogenous nucleation of the primary Mg_2Si. Because the precipitation of the $BaMg_2Si_2$ compound is fine and dispersed, the nucleation rate of the primary Mg_2Si significantly increases, inhibiting the growth of the primary Mg_2Si and obtaining grain refinement. At the same time, as the solidification proceeds, the excess unreacted Ba will be enriched at the front of Mg_2Si crystals growing together with the element of Er and inhibit the anisotropic growth of Mg_2Si crystals[26], which plays another role in refining Mg_2Si crystals.

So, the simultaneous addition of Er and Ba can play a synergistic role in modification of Mg_2Si. The element Ba can generate fine and dispersed crystal nuclei of $BaMg_2Si_2$ in the Mg-2.5Si-4Zn alloy melt as the core of the incipient Mg_2Si at the early stage of solidification of the alloy. In addition, the growth of primary and eutectic Mg_2Si is inhibited due to the strong enrichment of both Er and Ba on the surface of Mg_2Si crystal, which results in a better modification effect than the single modifier of Er.

In addition, when the Ba content is very high (larger than 0.8wt%), $BaMg_2Si_2$ crystal nucleus will undergo the growth under the enough composition condition and gradually grow into needle-like crystal. These needle-like $BaMg_2Si_2$ phases cannot become the heterogeneous nucleation core of the incipient Mg_2Si. The amount of $BaMg_2Si_2$ in the alloy melt as the heterogeneous nucleation core of Mg_2Si decreases, resulting in a weakened modification effect as an over-modified phenomenon.

2.3 Effect of Er and Ba modification on mechanical properties of Mg-2.5Si-4Zn alloy

The engineering stress-engineering strain curves of the Mg-2.5Si-4Zn-0.6Er alloys modified with different contents of Ba are shown in Fig. 14. It can be seen that the Er-Ba composite modification has a significant effect on the tensile strength and elongation of the Mg-2.5Si-4Zn alloy. The room-temperature mechanical properties of Mg-2.5Si-4Zn-0.6Er alloys with different Ba contents are shown in Fig. 15. It can be seen that when 0.8wt% of Ba is added into the Mg-2.5Si-4Zn-0.6Er alloy, its tensile strength σ_b and elongation δ reach the maximum of 168 MPa and 5.04%, respectively, and the tensile strength σ_b is increased by 14.3% compared with that of the Mg-2.5Si-4Zn alloy with 0.6wt% Er single modifier.

Under the condition of Er-Ba composite modification, the morphology of the primary Mg_2Si is effectively transformed into complex fine polygonal morphology with holes, while the size of eutectic Mg_2Si is also significantly reduced with more uniform and dispersed distribution, which makes the matrix of the magnesium alloy be strengthened by the fine Mg_2Si dispersion and the cutting effect of the coarse primary Mg_2Si on the alloy matrix weakened or even eliminated. Therefore,

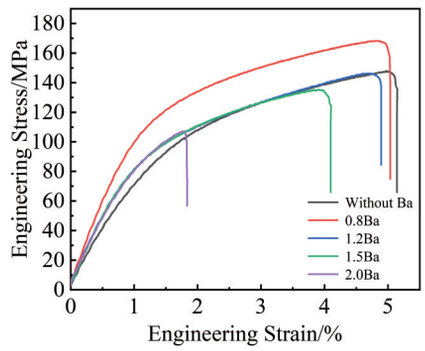

Fig. 14 Stress-strain curves of Mg-2.5Si-4Zn-0.6Er alloys with different Ba content

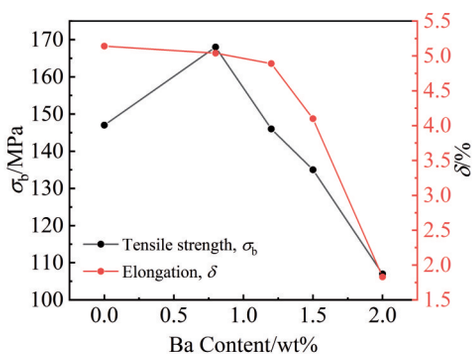

Fig.15 Tensile strength σ_b and elongation δ of Mg-2.5Si-4Zn-0.6Er alloys with different Ba contents

the tensile strength of the alloy increases markedly. But when the Ba addition is larger than 0.8wt%, the tensile strength of the alloy is contrarily smaller than that of the alloy only modified by the Er element. According to the above explanation, it presumably results from the weakening modification and the matrix cutting by the needle-like $BaMg_2Si_2$ phase (as shown in Fig.6f) in the alloy with higher Ba content.

Fig. 16 shows the SEM fracture morphology of the tensile specimens of the alloy, where Fig. 16a–16b show the tensile fracture of the specimen added with 0.8wt% Ba and Fig. 16c–16d shows the alloy added with 1.5wt% Ba.

It can be seen from Fig. 16a and 16b that the dark-grey smooth and flat area located in the white dotted ellipse (in Fig. 16b) on the fracture surface of the specimen (called "dimple") is the fracture morphology of the primary Mg_2Si, and the lamellar bright area formed by tearing is α-Mg (marked in Fig. 16b). The irregular smooth polyhedral or fine granular profile of the primary Mg_2Si, which can be considered as a kind of intergranular fracture morphology, is obviously the main component of the fracture morphology. But in Fig. 16d, there are some long tears inside the coarser primary Mg_2Si phase located in the white dotted ellipse (in Fig. 16d), indicating the transgranular fracture. Meanwhile, eutectic Mg_2Si cannot be observed on the fracture surface, suggesting that it does not act as a crack source during the fracture of the tensile specimen.

During the tensile process, the stress concentration will

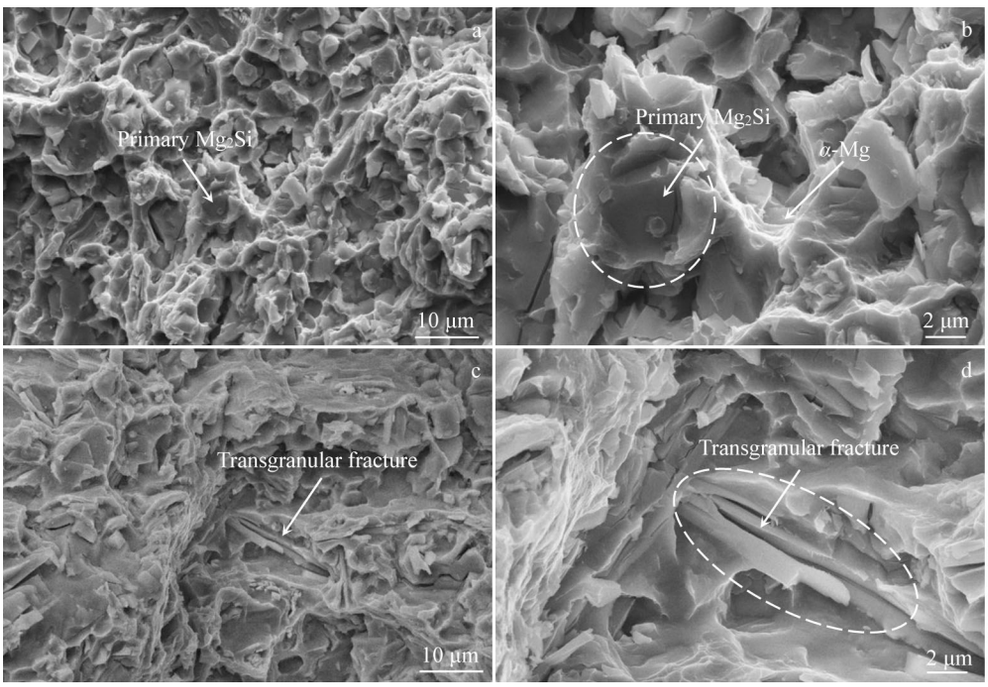

Fig.16 Details of fracture morphologies of Mg-2.5Si-4Zn-0.6Er alloy with different adding contents of Ba: (a–b) 0.8wt% and (c–d) 1.5wt%

occur at the primary Mg_2Si due to its characteristics of high hardness and high elastic modulus. If there are some holes and grooves mentioned above on the surface of primary Mg_2Si formed during the solidification of the alloy melt, they can be regarded as the defects of the primary Mg_2Si. The coarser the primary Mg_2Si, the more the above defects. When the stress concentrated on the defect is greater than the cracking condition of the alloy, the source of fracture at this location is the primary Mg_2Si itself, that is, transgranular fracture will occur (as shown in Fig. 16d). But when the shape of the primary Mg_2Si is regular polygonal or the stress at the defect is not sufficient to cause the primary Mg_2Si crystal to crack, the intergranular fracture will occur, only depending on a microcrack at the interface between the primary Mg_2Si and α-Mg, as shown in Fig. 16b. Compared with the fractures shown in Fig. 16c and 16d, there are a lot of dimples formed by the intergranular facture, increasing the tensile strength.

3 Conclusions

1) With increasing the addition of Er from 0wt% to 0.6wt% to Mg-2.5Si-4Zn alloy, the primary Mg_2Si in the alloy changes from coarse dendritic to regular tetragonal shape and the eutectic Mg_2Si changes from Chinese script to more complex short-rod shape. Moreover, the primary and eutectic Mg_2Si become small in size. But when the Er addition amount continues to increase to >0.6wt%, the size and morphology of the primary and eutectic Mg_2Si change back gradually. The best effect of Er modification is achieved when 0.6wt% of Er is added to the magnesium alloy.

2) With increasing the addition content of Ba within 0.8wt%, the primary Mg_2Si in the Mg-2.5Si-4Zn-0.6Er alloy is changed from a regular tetragonal block to an irregular polygonal block with holes and grooves and its size decreases a little, while the primary Mg_2Si gradually changes back to a coarse irregular dendritic shape and increases obviously in size when the Ba addition increases to above 0.8wt%. Moreover, the eutectic Mg_2Si is changed from a more complex short rod shape to a fine dot-rod shape with the increase in Ba addition and its size gradually decreases.

3) The modification of primary and eutectic Mg_2Si is the best when the 0.6wt% Er and 0.8wt% Ba are simultaneously added to the Mg-2.5Si-4Zn alloy, by which the primary Mg_2Si becomes an irregular polygonal block with the average area of about 124 μm^2 and the eutectic Mg_2Si has a simple dot-rod shape with an average area about 69 μm^2. The mechanical properties of the Mg-2.5Si-4Zn alloy are significantly improved after the Er-Ba composite modification and reach to the best values (tensile strength σ_b=168 MPa and elongation δ=5.04%, respectively) with the optimal adding contents of Er and Ba.

4) The simultaneous addition of Er and Ba can play a synergistic role in modification of Mg_2Si. The fine and dispersed $BaMg_2Si_2$ generated in the Mg-2.5Si-4Zn alloy melt at the beginning of solidification acts as the heterogeneous nucleation core for the primary Mg_2Si and the growth of primary and eutectic Mg_2Si is inhibited due to the strong enrichment of both Er and Ba on the surface of Mg_2Si crystal, which results in a better modification effect than the single modifier of Er.

References

1 Wu Guohua, Chen Yushi, Ding Wenjiang. *Manned Spaceflight*[J], 2016, 22(3): 281 (in Chinese)

2 Mordike B L, Ebert T. *Materials Science and Engineering A*[J], 2001, 302(1): 37

3 Dai Xiaojun, Yang Xirong, Wang Chang *et al. Rare Metal Materials and Engineering*[J], 2022, 51(12): 4421

4 Song Peiwei, Bai Mei. *Journal of Shaanxi University of Technology (Natural Science Edition)*[J], 2014, 30(3): 10 (in Chinese)

5 Huang Zhenghua, Guo Xuefeng, Zhang Zhongming *et al. Journal of Materials Engineering*[J], 2004, 6: 28 (in Chinese)

6 Li C, Wu Y Y, Li H *et al. Acta Materialia*[J], 2011, 59(3): 1058

7 Yang Mingbo, Pan Fusheng, Zhang Jing. *Foundry Technology*[J], 2005, 26(4): 331 (in Chinese)

8 Lotfpour M, Emamy M, Allameh S H *et al. Procedia Materials Science*[J], 2015, 11: 38

9 Cong Mengqi, Li Ziquan, Liu Jinsong *et al. Journal of Alloys and Compounds*[J], 2012, 539: 168

10 Salasel A R, Abbasi A, Barri N *et al. Materials Chemistry and Physics*[J], 2019, 232: 305

11 Mosleh S, Emamy M, Majdi H *et al. Procedia Materials Science*[J], 2015, 11: 79

12 Tsuzuki R, Kondoh K. *Materials Science Forum*[J], 2005, 475(1): 497

13 Sheng Shaoding, Pan Chengling, Wang Qingping. *Hot Working Technology*[J], 2012, 41(10): 125 (in Chinese)

14 Tsuzuki R, Kondoh K, Du W *et al. Materials Science Forum*[J], 2003, 419(2): 789

15 Li Yaohui, Li Ke, Yin Wenlai *et al. Rare Metal Materials and Engineering*[J], 2022, 51(1): 266 (in Chinese)

16 Tong Wenhui, Zhao Chenxi, Tong Fangze *et al. Rare Metal Materials and Engineering*[J], 2022, 51(12): 4410

17 Geng Peng, Jin Peipeng, Wang Mingliang *et al. Foundry Technology*[J], 2015, 36(2): 399 (in Chinese)

18 Srinivasan A, Ningshen S, Kamachi Mudali U *et al. Intermetallics*[J], 2007, 15(12): 1511

19 Yang Mingbo, Pan Fusheng, Bai Liang *et al. Chinese Journal of Nonferrous Metals*[J], 2007, 17(12): 2010 (in Chinese)

20 Song Haining, Yuan Guangyin, Wang Qudong *et al. The Chinese Journal of Nonferrous Metals*[J], 2002, 12(5): 956 (in Chinese)

21 Liu Hui. *Effect of Modification on Microstruture and Mechanical Properties of Hypereutectic Mg-5Si Alloy*[D]. Nanchang: Nanchang Hangkong University, 2014 (in Chinese)

22 Jiang Q C, Wang H Y, Wang Y *et al. Materials Science and Engineering A*[J], 2005, 392(1): 130

23 Huang Xiaofeng, Wang Qudong, Liu Liufa *et al. Rare Metal Materials and Engineering*[J], 2005, 34(5): 795 (in Chinese)

24 Ghandvar H, Jabbar K A, Idris M H *et al. Journal of Materials Research and Technology*[J], 2021, 11: 448

25 Chen Ke, Li Ziquan. *Journal of Alloys and Compounds*[J], 2014, 592: 196

26 Tong Wenhui, Liu Yulin, Liu Yukun *et al. The Chinese Journal of Nonferrous Metals*[J], 2019, 29(1): 27 (in Chinese)

27 Cui Ce, Yao Junping, Zhang Lei *et al. Special-cast and Nonferrous Alloys*[J], 2017, 37(11): 1238 (in Chinese)

28 Bai Shimei, Yao Junping, Liao Luliang. *Special-cast and Nonferrous Alloys*[J], 2016, 36(12): 1337 (in Chinese)

29 Bramfitt B L. *Met Trans*[J], 1970, 1(7): 1987

30 Hu Bo, Zhu Wenjie, Li Zixin *et al. Journal of Magnesium and Alloys*[J], 2021, 2213: 9567

31 Chen Ke, Li Ziquan, Liu Jinsong *et al. Journal of Materials Engineering*[J], 2010, 24(4): 63 (in Chinese)

Er-Ba复合变质对Mg-2.5Si-4Zn铸造合金组织及性能的影响

童文辉，黄博男，孙博玮，王　杰，白宇飞

(沈阳航空航天大学 材料科学与工程学院，辽宁 沈阳 110136)

摘　要：镁合金中的强化相Mg_2Si可以显著提高合金的硬度、耐磨性，特别是耐高温蠕变性。但铸态过共晶Mg-Si合金中初生Mg_2Si棱角粗糙，共晶Mg_2Si具有复杂的汉字形态，会严重割裂合金基体。为了改善Mg-2.5Si-4Zn合金的性能，进行了添加Er/Er-Ba的变质实验，并通过光学显微镜（OM）、扫描电子显微镜（SEM）、能量色散光谱仪（EDS）和X射线衍射仪（XRD）研究了Er/Er-Ba对合金组织和Mg_2Si相的影响。利用计算机辅助电子加载拉伸试验机对力学性能进行了测试和分析。结果表明，在Mg-2.5Si-4Zn合金中加入0.6%（质量分数）的Er，其组织中的初生Mg_2Si从粗大的树枝状转变为规则的四方块状，而共晶Mg_2Si则从粗大的汉字状转变为更复杂的短棒状。随后加入0.8%的Ba后，初生Mg_2Si从规则的四边形块状进一步转变为带有沟槽和孔洞的不规则细小块状，共晶Mg_2Si在尺寸上细化效果显著，呈点线状弥散分布在合金基体中。当加入0.6%Er和0.8%Ba时，变质效果最佳。经Er-Ba复合变质的Mg-2.5Si-4Zn合金的力学性能得到显著改善，抗拉强度σ_b和伸长率δ分别提高到168 MPa和5.04%。

关键词：Mg-Si-Zn合金；Mg_2Si；组织；复合变质；力学性能

作者简介：童文辉，男，1971年生，博士，副教授，沈阳航空航天大学材料科学与工程学院，辽宁 沈阳 110136，电话：024-89728968，E-mail：20140013@sau.edu.cn